ChemEurJ

Research Article
doi.org/10.1002/chem.202502853

Chemistry Europe
European Chemical Societies Publishing

www.chemeurj.org

Acyclic Nucleoside Phosphonates As Potential Inhibitors Of *Plasmodium Falciparum* Egress

Thomas Cheviet,*[a] Sharon Wein,[b] Corinne Lionne,[c] Yan Badji,[a] Natacha Venturini,[a] Rachel Cerdan,*[b] and Suzanne Peyrottes*[a]

In memory of Prof. Frank Seela

The emergence of drug-resistant Plasmodium strains requires the development of novel antimalarial agents with original mechanisms of action. Here, we report the synthesis and biological evaluation of a new family of nucleotide analogues aiming to target an essential step of the development of the malaria parasite. Two series of acyclic nucleoside phosphonates were designed to incorporate strategic structural modifications either on the purine scaffold or on the acyclic chain. All synthesized compounds were evaluated against chloroquine-sensitive (3D7) Plasmodium falciparum strains. A few compounds demonstrated in vitro antimalarial activity with IC_{50} values ranging from 11.3 to38.8 µM. In addition, a molecular docking study revealed some crucial interactions with the putative target and supports the biological data. The present study establishes this novel family of nucleotide analogues as promising antimalarial scaffolds, warranting further optimization and evaluation.

1. Introduction

Malaria is one of the most ancient diseases and the deadliest parasitic disease, causing thousands of deaths each year (5,97,000 in 2023, according to WHO, for 263 million cases worldwide),[1] mostly in subequatorial countries. It is caused by a parasite of the *Plasmodium* genus (a unicellular eukaryote organism) transmitted to humans by *Anopheles* mosquitoes during their blood meals. Six known species of *Plasmodium* are able to infect humans, the most widespread and deadly being *Plasmodium falciparum*. Parasites delivered in the bloodstream infect red blood cells (RBC), where they replicate asexually and form up to 32 daughter cells (merozoites), which actively exit the host cell, a process called egress, to invade new RBCs. Symptoms are commonly fever, anemia, and nauseas and can go until coma or death. Current treatments such as chloroquine or ACTs (artemisinin combination therapies) are facing a considerable resistance phenomenon throughout the globe,[2–4] and the search for new antimalarial treatments and/or new targets is considered a priority. Among the investigated alternatives, vaccines such as the approved RTS, S/AS01 (Mosquirix, GSK) have been developed and administered in African countries but show several secondary effects, have moderate and short-term efficiency, and require injection of several doses, storage at low temperature and qualified people to be administrated. [5–7] The WHO recently recommended a second malaria vaccine, R21, to complement the ongoing rollout of RTS, S/AS01. Hence, a low-cost, per *os* administered, and easy-to-transport small molecule-based treatment would still be the best alternative.

[a] *T. Cheviet, Y. Badji, N. Venturini, S. Peyrottes*
Pole Recherche Balard, Institute for Biomolecules Max Mousseron (IBMM), Univ. Montpellier, CNRS, ENSCM, Nucleosides & Phosphorylated Effectors, 1919 route de Mende, Montpellier 34293, France
E-mail: thomas.cheviet@hotmail.fr
suzanne.peyrottes@umontpellier.fr

[b] *S. Wein, R. Cerdan*
Laboratory of Pathogens and Host Immunity (LPHI), Univ. Montpellier, CNRS, INSERM, Place E. Bataillon, Montpellier 34095, France
E-mail: rachel.cerdan@umontpellier.fr

[c] *C. Lionne*
Centre de Biologie Structurale (CBS), Univ. Montpellier, CNRS, INSERM, 29 rue de Navacelles, Montpellier 34090, France

Abbreviations: AcOEt, ethyl acetate; AcOH, acetic acid; AMP, adenosine 5′-monophosphate; ANP, acyclo-nucleoside phosphonate; Boc, tert-butyloxycarbonyl; cGMP : 3′,5′, cyclic-guanosine monophosphate; DEAD, diethyl azodicarboxylate; DIAD, diisopropyl azodicarboxylate; DEP, diethyl phosphite; DIEA, diisopropylethylamine; DMF, N,N-dimethylformamide; DMSO, dimethyl sulfoxide; DMTr, 4,4′-dimethoxytrityl; DPAP, 2,2-dimethoxy-2-diphenylacetophenone; ESI, electrospray ionization; GC, guanylate cyclase; H-Asp-OH, aspartic acid; H-Glu-OH, glutamic acid; HGXPRT, hypoxanthine-guanine-xanthine phosphoryl transferase; HPLC, high performance liquid chromatography; HRMS, high resolution mass spectrometry; IC_{50}, concentration required for 50% of inhibition of the parasite growth; LiHMDS, lithium bis(trimethylsilyl)amide; MamAC, mammalian adenylate cyclase; Me, methyl; MeOH, methanol; n-BuLi, n-butyllithium; NMR, nuclear magnetic resonance; N,O-BSA, N,O-bis(trimethylsilyl)acetamide; NPP, new permeation pathways; pD, pH in deuterated media; PE, petroleum ether; Pf, Plasmodium falciparum; RP, reverse phase chromatography; TFA, trifluoroacetic acid; THF, tetrahydrofuran; TLC, thin layer chromatography; TMSBr, trimethylsilyl bromide; UV, ultra violet.

Supporting information for this article is available on the WWW under https://doi.org/10.1002/chem.202502853

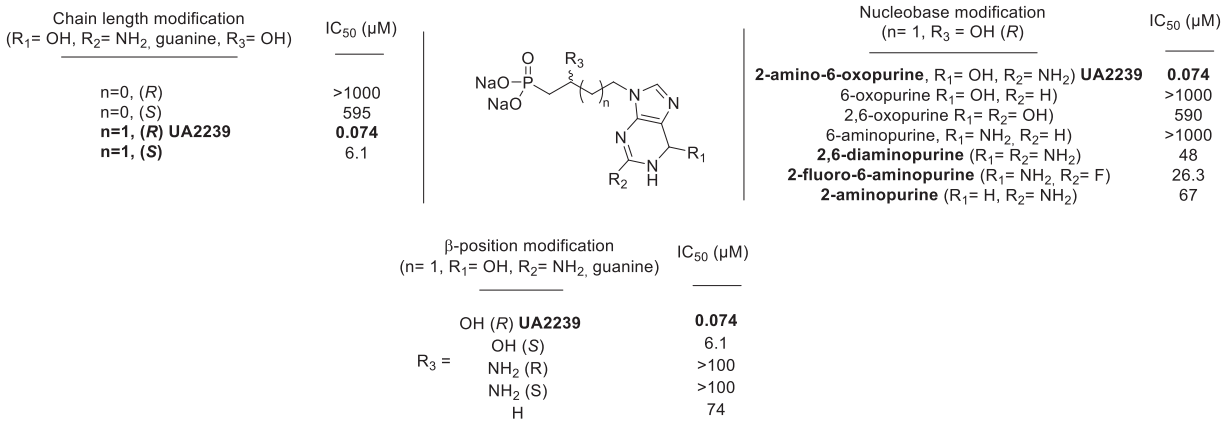

Figure 1. Structures of some relevant compounds previously studied.[14]

Acyclic nucleoside phosphonates (ANPs), historically used as antivirals,[8] are also known since the 90 s as inhibitors of in vitro growth of *Plasmodium falciparum*[9] and have been essentially developed against parasitic hypoxanthine-guanine-xanthine phosphoribosyl transferase (HGXPRT, the believed target of such family of compounds) for many years.[10–13] Thus, the HGXPRT is involved in the purine salvage pathway, which the parasite relied on entirely to produce its own genetic material. In our previous study, the synthesis of a novel series of ANPs and their subsequent biological evaluation in *Pf*-infected RBCs led us to identify a very promising hit (named UA2239, Figure 1) exhibiting nanomolar range IC_{50} value.[14] We initially hypothesized that the target was *Pf* HGXPRT but discovered afterwards that the development of the parasite, including the formation of merozoites, was not impacted. Furthermore, the absence of newly infected RBCs, combined with the continued accumulation of late-stage parasites, suggests that the compound's mechanism of action inhibits parasite egress from the RBCs.[14] Indeed, we recently characterized the mechanism of action of UA2239, which impairs parasite egress by reducing cGMP levels.[15]

To our knowledge, no nucleotide or nucleoside analogues have been described in the literature as inhibitors of the malaria parasite egress. This groundbreaking observation convinced us to extend our SAR study by synthesizing new analogues of UA2239. Compounds were prepared from a diversity point of view in order to further probe the active scaffolds, including modification of the purine moiety and of the chain moiety (Figure 2). Herein, we report on the preparation of novel acyclic nucleoside phosphonates and their biological evaluation in in vitro assays using *Pf*-infected red blood cells, as well as data from a docking study with their putative target.

2. Results and Discussion

2.1. Chemistry

On the basis of the structure of UA2239, we pursued the SAR studies by replacing the guanine by 6-modified-2-aminopurines and 7-deazaguanines (Figure 2, compounds **1** to **4**). Isosteric replacement of oxygen with sulfur is well-known in medicinal chemistry and especially in the family of purine derivatives (i.e., 6-mercaptopurine and 6-thioguanine). The sulfur analogs are often more resistant to oxidative metabolism, potentially leading to improved pharmacokinetic profiles. In addition, as the compound containing 2-fluoro-6-aminopurine (Figure 1) has already shown moderate activity, a derivative bearing 2-fluoro-6-oxopurine was also synthesized (compound **5**). As we previously studied β-hydroxyphosphonates, including propyl (C3) et butyl (C4) chain length, two compounds including a pentyl (C5) chain length have been prepared (β- and γ- hydroxyphosphonates **6** and **7**). Then, to investigate more thoroughly the importance of the hydroxyl group of the acyclic chain, it was either replaced by a carbonyl (compound **8**), a phosphonic acid (compound **9**), as bisphosphonate derivatives have already been shown to be of interest,[16–18] a diol group (in order to enhance the potential polar interaction with the target) to form α, β-bis-hydroxyphosphonates (**10**) or a β, γ-bis-hydroxyphosphonates (**11**). This last derivative requiring the preparation of an allyl phosphonate intermediate, we also took the opportunity to obtain the corresponding unsaturated derivative (**12**). The structure of bis-hydroxylated and bis-phosphonylated compounds could enhance the number of interactions between the compound and the target, whereas the oxidation of the hydroxyl led to the loss of the chiral center and of the hydrogen-bound donor character, which could result in a modification of the interaction with the protein.

As the *R*-isomers displayed the best biological activities in our previous report,[14] this feature was not modified on the newly synthesized compounds (except in the case of the compounds containing the γ-hydroxy-butyl chain, the β-keto, or the diol functionality).

Thus, synthetic pathways for modified nucleobase derivatives (scheme 1) were adapted from our previous work.[14] At first, the desired nucleobases **13a-c** were protected beforehand with Boc groups on exocyclic amines from commercially available 2-amino-6-chloropurine, 2-amino-7-deaza-6-chloro- or 6-methoxy-purine to avoid side reactions. The 2-fluoro-6-methoxypurine **13d** was obtained from commercially available 2-amino-6-methoxypurine (nitrous deamination in the presence of HBF_4.) as described in the literature.[19]

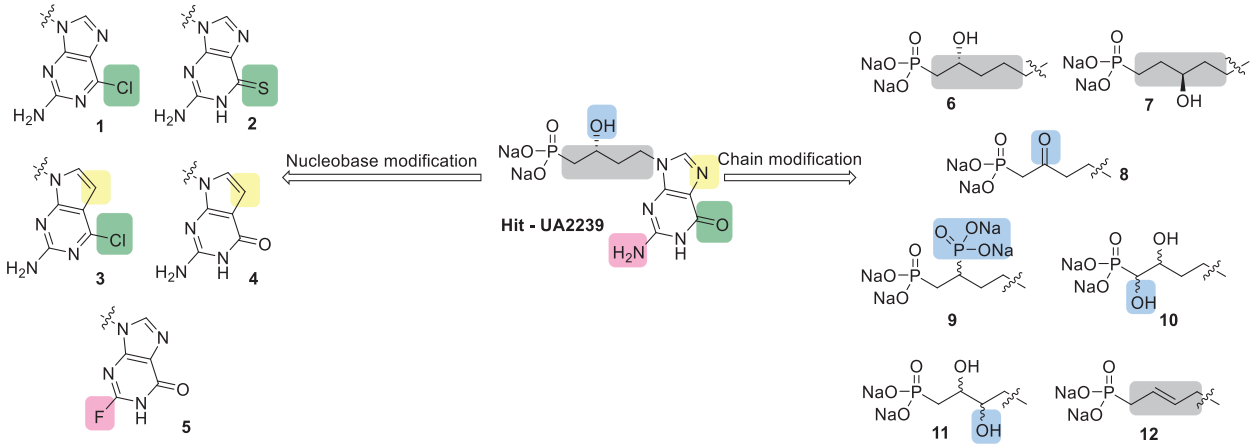

Figure 2. Overall view of the planned modifications of UA2239.

All nucleobase derivatives **13a-d** were coupled to the 2-hydroxyethyloxirane, which was prepared in three steps starting from L-aspartic acid according to our previous report,[14] in Mitsunobu conditions, affording the *N*-9 alkylated compounds **14a-d** (as major regioisomers for derivatives **14a** and **14d**, identified with ^{1}H-^{13}C HMBC analysis). Minor *N-7* isomers were not isolated pure enough to be fully characterized).

Then ring-opening of the epoxides was achieved with the nucleophilic addition of lithiated diethyl phosphite. The obtained β-hydroxyphosphonate derivatives **15a-c** were treated with trifluoroacetic acid and then bromotrimethylsilane (for **15d**) to afford the corresponding fully deprotected phosphonic acid after purification by reverse-phase chromatography on C18-grafted silica gel. For the 6-chloro-purine analogues (**16a-b**), 2,6-lutidine had to be used to avoid any side reactions on the chlorinated nucleobase (such as trans halogenation) during treatment with bromotrimethylsilane. Then, percolation of the compounds onto an ion-exchange resin (Na^+ form) led to the water-soluble sodium salt **1–5**.

The synthesis of 2-amino-6-thiopurine derivative **2** was performed using the 2-amino-6-chloropurine intermediate **15a** through refluxing in ethanol in the presence of sodium hydrosulfide, followed by the usual deprotection and hydrolysis steps to afford the corresponding sodium salt with excellent yields. Synthesis of fluorinated derivative **5** was achieved from intermediate **15d** following similar deprotection steps.

Synthetic routes to compounds including a pentyl (C5) chain length, compounds **6** and **7**, are presented in scheme 2. Preparation of the C5-β-hydroxyphosphonate compound **6** required to start all the way back from *L*-glutamic acid, rather than *L*-aspartic acid, on which similar conditions were applied to obtain bromodiol **17**.[20] This last was treated in the presence of Cs_2CO_3, affording the 2-hydroxypropyloxirane which is in situ coupled with the 6-methoxy-2-(di-Boc)-aminopurine (synthesized beforehand from the commercially available 6-methoxy-2-aminopurine according to a previously published procedure)[14] in Mitsunobu conditions. Thus, intermediate **18** is isolated in moderate yield and then submitted to the nucleophilic addition of silylated diethyl phosphite to afford the corresponding β-hydroxyphosphonate **19**. The lower yield should be attributed to the decreased reactivity of the epoxide toward nucleophiles since the electron-withdrawing nucleobase is farther than for the C4 compound series.

The C5-γ-hydroxyphosphonate derivative **7** was synthesized starting from epoxide **20**, whose synthesis is described in our previous study (scheme 2).[14] The ring-opening reaction was performed in the presence of the methyl diethylphosphonate treated with *n*-BuLi. Initial conditions tested involved 3 equivalents of Lewis acid $BF_3.Et_2O$, at -78 °C to room temperature for 2 hours, but low yields were observed due to side reactions involving the nucleophilic addition of methyl diethylphosphite on the carbamate moiety. Consequently, reaction time was shortened to 1.5 hours, and the mixture was kept at -78 °C, then 7 eq. of $BF_3.Et_2O$ were added to afford compound **21** with 53% yield. Removal of the protecting groups from **19** and **21** was performed with the standard procedure involving TFA in CH_2Cl_2, then TMSBr in DMF, followed by percolation on Dowex Na^+ ion exchange resin to afford the desired compounds **6** and **7**.

The synthetic route to β-ketophosphonate compound **8** was adapted from a described procedure,[21,22] and was achieved starting from the nucleophilic addition of 2-amino-6-methoxypurine on benzyl acrylate as the Michael acceptor in the presence of diisopropylethylamine (DIEA) with moderate yield (scheme 3). The exocyclic amine of the *N*-9 alkylated compound **22** (no traces of *N*-7 isomer was observed) was then protected with a 4,4′-dimethoxytrityl group to avoid side reactions and to enhance the substrate solubility in organic solvents. Addition of dimethyl methylphosphonate (DMMP, dried over KOH and distilled), treated beforehand with *n*-BuLi, was then performed on the benzylic ester (with concomitant elimination of the benzyl alkoxide) to afford compound **23** in poor yield. Indeed, the purification step was quite laborious, and the protected purine was also recovered as a side product. Then treatment of **23** with TFA in CH_2Cl_2, then TMSBr in the presence of 2,6-lutidine, followed by percolation on Dowex Na^+ ion exchange resin, afforded the desired compound **8** with low yield. Obviously, the presence of 2,6-lutidine during the last step of the synthesis involving bromotrimethylsilane was not sufficient to avoid side reactions occurring on the reactive carbonyl moiety.

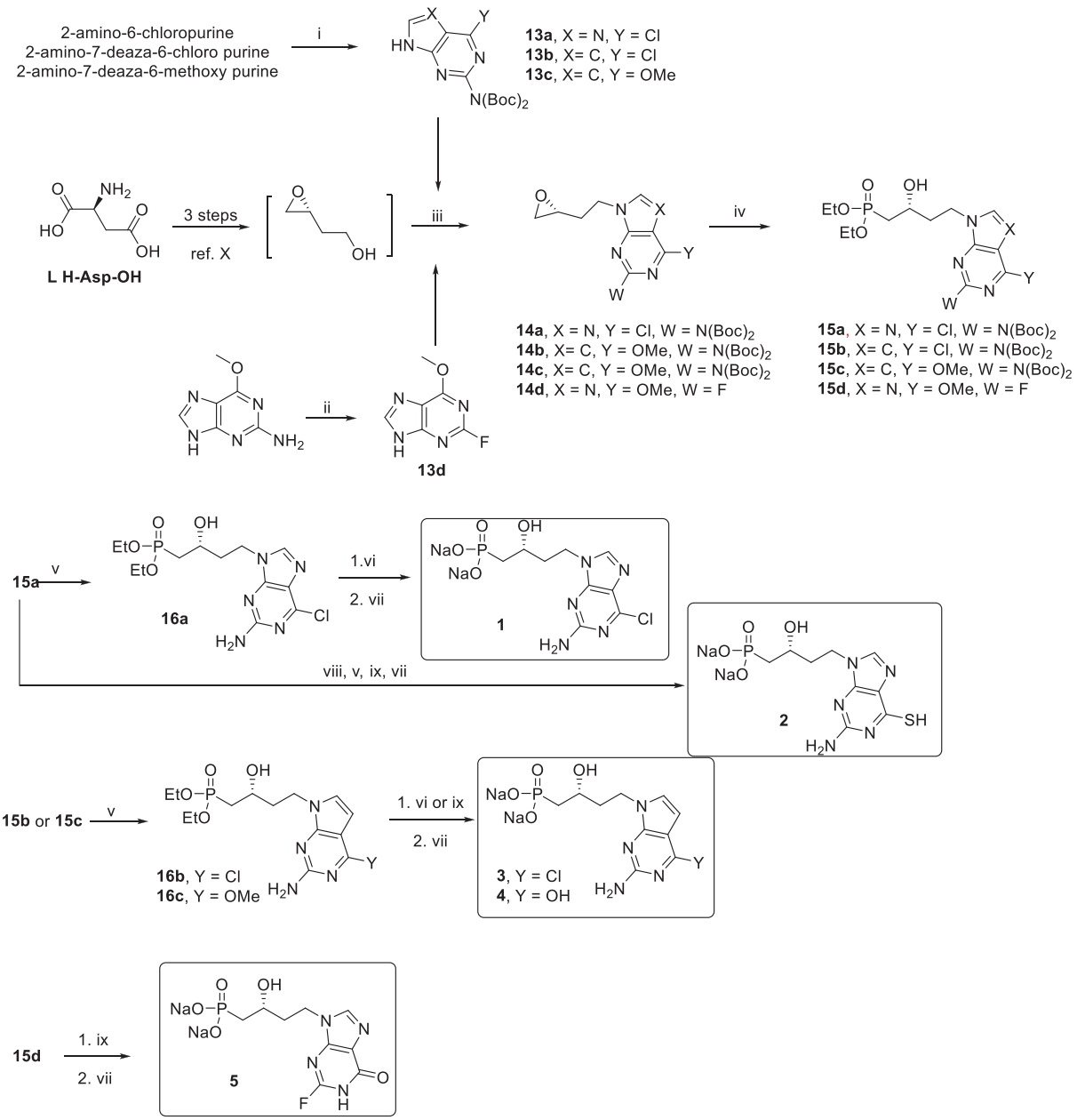

Scheme 1. Synthetic route to nucleobase-modified compounds 1 to 5.[a]

[A] Reagent and conditions: (i) Boc_2O, DMAP, THF, rt, overnight, then $NaHCO_3$ aq. (sat.) in MeOH (for 13a) or MeONa in THF/MeOH (for 13b-c), 56–98%; (ii) $NaNO_2$, HBF_4, water, -20 °C to rt, 3 hours, 55%; (iii) PPh_3, DIAD, THF, rt, overnight, 40–94%; (iv) DEP, *N,O*-BSA, THF, reflux 4 hours, then epoxide, $BF_3.Et_2O$, THF, -60 °C, 2 hours, then to overnight, rt, 19–77%; (v) TFA/CH_2Cl_2, rt, 1 hours, 29–98%; (vi) TMSBr, 2,6-lutidine, DMF, rt, overnight, then MeOH, rt, 20 minutes (for 1 and 3), then (vii) Dowex Na^+, 50–61%; (viii) NaSH in EtOH, EtOH, reflux, 2 hours, 93%; (ix) TMSBr, DMF, rt, overnight, then MeOH, rt, 20 minutes, (for 2, 4 and 5), then (vii), 37–65%.

Both bis-phosphonylated derivative **9** and the racemic mixture of α, β-bis-hydroxyphosphonate derivative **10** were obtained from the vinyl phosphonate derivative **24** (scheme 4). This last was synthesized in two steps starting with the radical hydrophosphonylation of 3-butyn-1-ol in the presence of diethyl phosphite and 2,2-dimethoxy-2-phenylacetophenone (DPAP) as a photo-initiator under UV irradiation, followed by a Mitsunobu coupling step with the protected nucleobase.[14] Surprisingly, the *Z* isomer (identified by NMR studies) was isolated as the major compound.

Thus, Michael's addition of diethylphosphite in the presence of sodium hydride onto intermediate **24** afforded the α, β-bisphosphonate derivative **25**. One should note that the treatment with DEP/NaH led to the cleavage of one Boc group (the instability of bis-Boc group toward nucleophilic addition was already observed in the presence of DEP/LiHMDS).[14] Compound **25** was then engaged in the usual deprotection steps (TFA in CH_2Cl_2, then TMSBr), and percolation on Dowex Na^+ ion exchange resin afforded the desired compound **9** as a sodium salt.

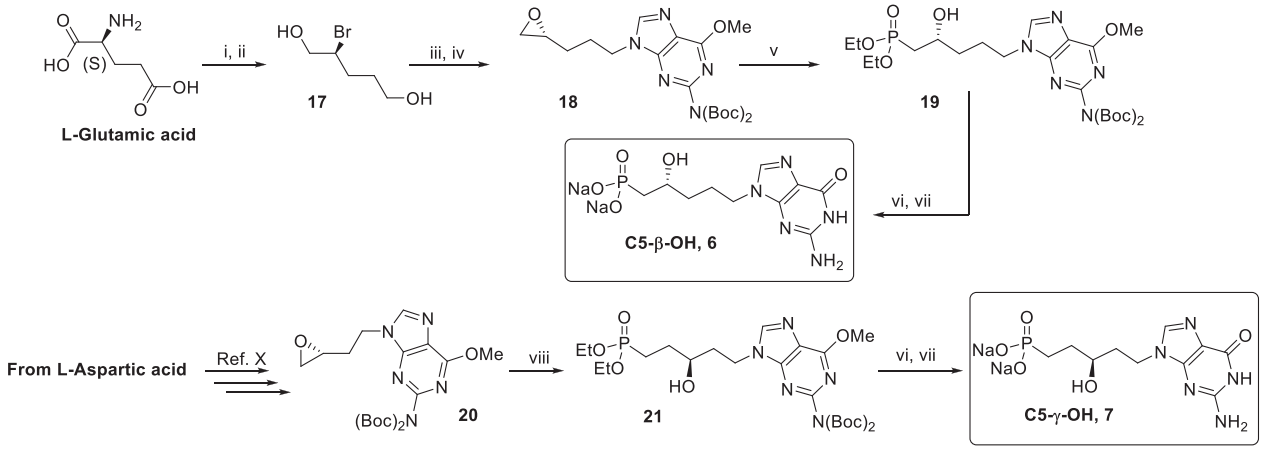

Scheme 2. Synthetic route to C5 chain length analogues 6 and 7.[a]
[A] Reagent and conditions: (i) $NaNO_2$/KBr/HBr, H_2O, -15 °C to rt, 4 hours, 42%; (ii). BH_3.THF, 0 °C to rt, 1.5 hours, 86%; (iii) Cs_2CO_3, CH_2Cl_2, overnight, rt; (iv) PPh_3, DEAD, 6-methoxy-2-(di-(*tert*-butoxycarbonyl))-aminopurine, THF, rt., 5 hours, 31% (over the 2 steps); (v) DEP, *N,O*-BSA, CH_2Cl_2, reflux, 4 hours, then epoxide **18**, $BF_3.Et_2O$, THF, -78 °C to rt, overnight, 70%; (vi) TFA/CH_2Cl_2, rt, 1 hour, 96–99%; (vii) TMSBr, DMF, rt, overnight, then MeOH, rt, 20 minutes. then Dowex Na^+ 27–65%; (viii) methyl diethylphosphite, *n*-BuLi, THF, -78 °C, 30 minutes, then epoxide **20**, $BF_3.Et_2O$, THF, -78 °C, 1.5 hours, 53%.

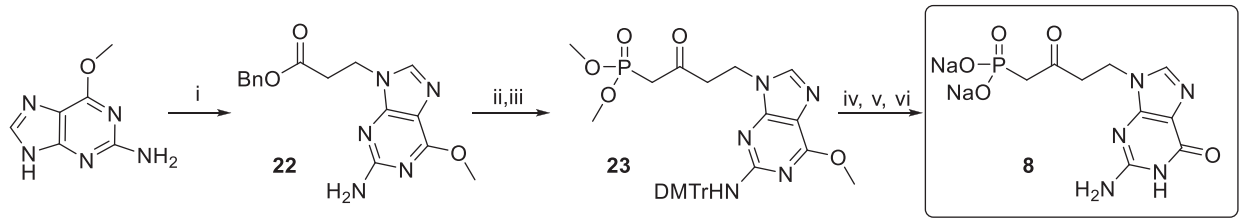

Scheme 3. Synthesis of β-ketophosphonate Derivative 8.[a]
Reagent and conditions: (i) Benzyl acrylate, DIEA, DMF, 80 °C, 4 days, 54%; (ii) DMTrCl, pyridine, rt., 1 day, 90%; (iii) DMMP, *n*-BuLi, THF, -78 °C, 3 hours, 24%; (iv) TFA/CH_2Cl_2, 10 minutes, rt, quant.; (v) TMSBr, 2,6-lutidine, DMF, rt, 1 day, then MeOH, rt, 20 minutes, (vi) Dowex Na^+ resin, 22% (over 2 steps).

The α, β-bis-hydroxyphosphonate derivative **26** was obtained as a racemic mixture using Sharpless dihydroxylation conditions from the vinyl phosphonate derivative **24**. Then, acidic treatment and diethylphoshonate deprotection step were performed to afford the final compound **10**. AD-mix-α and AD-mix-β were both tested, in the eventuality of obtaining slightly different enantiomeric excess between the two catalysts. However, the chiral selectivity given by the use of AD-mix reagent is reported not to be efficient on di-substituted olefins,[23] and we expected to obtain racemic mixtures. To check this, a nondestructive low-temperature ^{31}P NMR method of enantiomeric discrimination involving β-cyclodextrin and a controlled pD value was used, according to a previously published procedure.[14] In such conditions, enantiomers will exhibit different δ shifts and a length correlated to the ratio of each enantiomer. As shown in Figure 3, both spectra are closely identical, and both mixtures displayed two distinctly separated and same-length peaks, indicating that each is racemic.

The allyl phosphonate derivative **12** was obtained in four steps from *cis*-2-butene-1,4-diol (scheme 5). At first, a metathesis reaction with Grubbs 2nd generation catalyst between diethyl allylphosphite and the *cis*-2-butene-1,4-diol was carried out, and a mixture of *E*/*Z* isomers **27** (ratio 7:3) was obtained. They were separated by silica gel chromatography and identified by NMR studies.[24] The *E* isomer was then submitted to the usual sequence of reaction (Mitsunobu coupling leading to compound *E*-**28** and subsequent deprotection steps) to afford compound *E*-**12**.

Starting from compound *E*-**28**, the β,γ-bis-hydroxyphosphonate derivative **11** was obtained as a racemic mixture in three steps, including the Sharpless dihydroxylation in the presence of AD-mix β (compound **29**, scheme 5), followed by the removal of the protecting groups. In this case, only one AD-mix-β reagent was used since we already knew that it does not lead to enantioselectivity.

The straightforward synthesis of enantiomerically pure β-γ-bis-hydroxylphosphonate compounds **11a** and **11b** was also envisaged starting from the commercially available (+)-2,3-*O*-isopropylidene-*L*-threitol and (-)-2,3-*O*-isopropylidene-*D*-threitol, thus avoiding regio- and stereo-selectivity problems (scheme 6). The first step involved the introduction of the protected nucleobase in Mitsunobu conditions, and using (+)-2,3-*O*-isopropylidene-*L*-threitol as a starting material, leading to compound **30a**, then the substitution of the remaining alcohol was performed using iodine and triphenylphosphine in THF in the presence of imidazole. Substitution of the iodine from compound **31a** with diethyl phosphite previously treated by LiHMDS led to the expected phosphonate derivative **32a**. The last steps

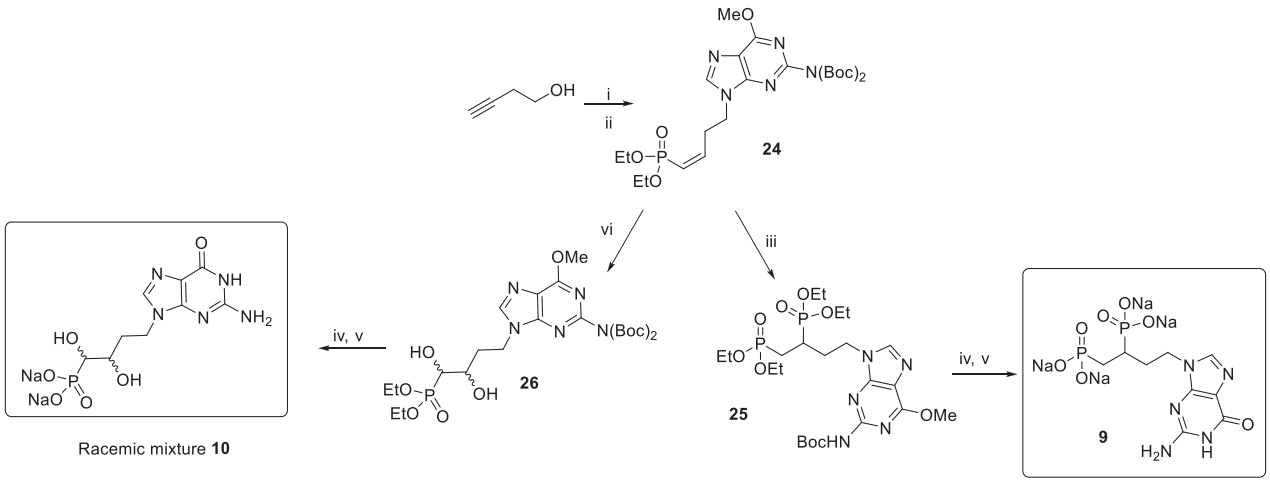

Scheme 4. Synthetic route to bis-phosphonylated and α, β-bis-hydroxyphosphonates, compounds 9 and 10.[a]
[A] Reagent and conditions: (i) DEP (50 eq.), DPAP (cat.), hν (365 nm, 60 W), 30 minutes, quant.; (ii) 2-(bis(Boc))amino-6-methoxypurine, PPh_3, DEAD, CH_2Cl_2/Et_2O, rt, overnight, 55%; (iii) DEP, NaH, THF, 0 °C, 30 minutes then **24** in THF, rt, overnight, 70%; (iv) TFA/CH_2Cl_2, rt, overnight, 90% to quantitative; (v) TMSBr, DMF, rt, overnight, then MeOH, rt, 20 minutes; then Dowex Na^+ resin, 62–66%; (vi) AD-mix α or β, $K_2OsO_4.2H_2O$, *t*BuOH, $CH_3SO_2NH_2$, H_2O, rt, 3 hours, 75%.

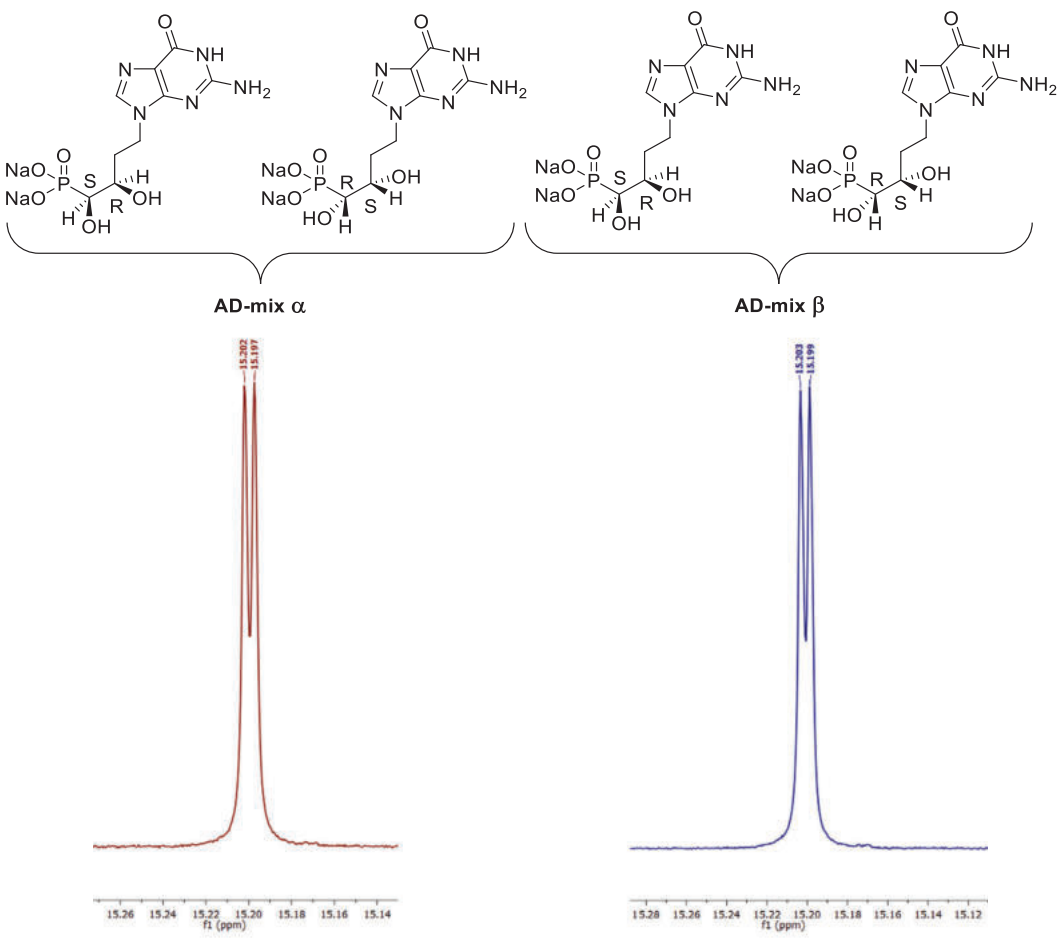

Figure 3. Comparison of ^{31}P NMR spectra of the mixtures of compounds 10a/10b obtained with AD-mix α or AD-mix β.[a]
[a] In red: racemic mixture obtained with AD-mix α. In blue, a racemic mixture is obtained with AD-mix β. Ppm is used as a shifts unit. NMR spectra were obtained at 15 °C in D_2O using NaOD addition to reach pD 11.8.

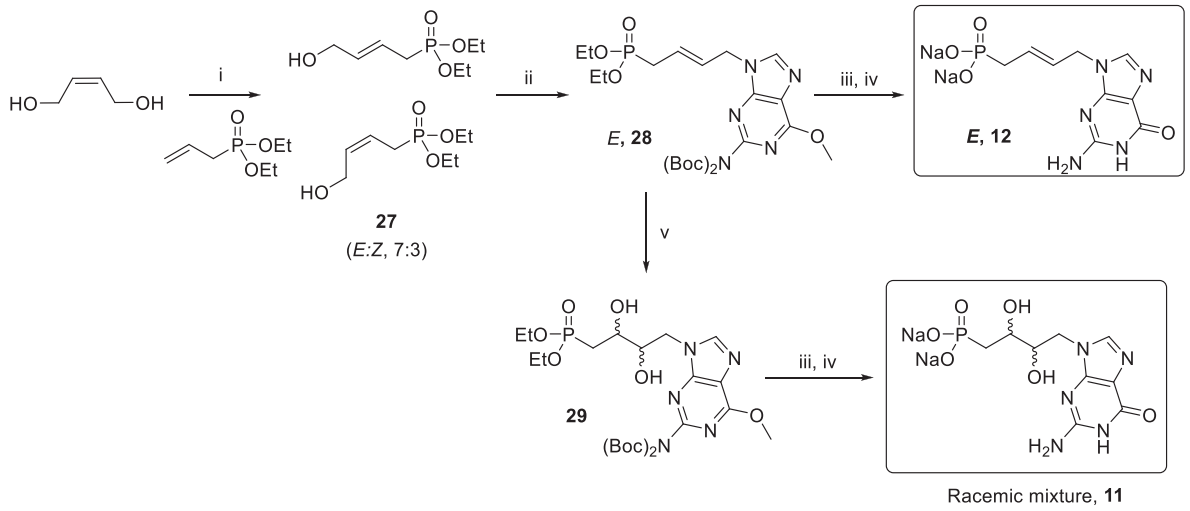

Scheme 5. Synthetic route to β,γ-bis-hydroxyphosphonate and allyl phosphonate containing compounds 11and 12.[a]
[A] Reagent and conditions: (i) Grubbs 2nd generation, CH_2Cl_2, 40 °C, 43% *E*, 19% *Z*; (ii) PPh_3, DIAD, CH_2Cl_2/Et_2O, 6-methoxy-2-(di-(*tert*-butoxycarbonyl))-aminopurine, 50%; (iii) TFA/CH_2Cl_2, rt, 95% to quantitative; (iv) TMSBr, DMF, rt then MeOH, rt, 20 minutes; then Na^+ resin, 66–84%; (v) AD-mix-β, $K_2OsO_4.2H_2O$, tBuOH, $CH_3SO_2NH_2$, H_2O, rt, 2 days, 21%.

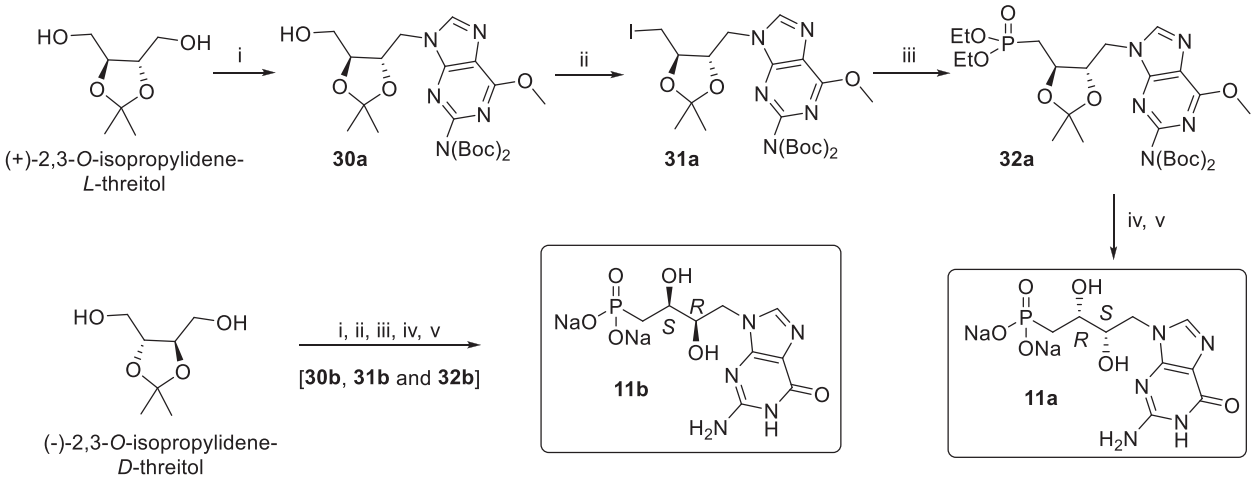

Scheme 6. Synthetic route to enantiomerically pure diol-containing compounds 11a and 11b.[a]
[A] Reagent and conditions: (i) PPh_3, DIAD, THF, rt, overnight, 65–81%; (ii) I_2, PPh_3, imidazole, THF, rt, overnight, 46–60%; (iii) DEP, LiHMDS (1 M in THF), THF, -78 °C, 15 minutes, then 31a or 31b in THF, -78 °C to rt, overnight, 60–74%; (iv) TFA/AcOH in H_2O, rt, overnight, 82–97%; (v) TMSBr, DMF, rt, overnight, then MeOH, 20 minutes, then Dowex Na^+ resin, 73–75%.

of the synthesis correspond to the removal of the acetal and Boc protecting groups using a mixture of TFA and acetic acid in water and finally cleavage of the phosphonate diester by treatment with bromotrimethylsilane, affording the enantiomerically pure compound **11a**. The same sequence of reactions was reproduced starting from (-)-2,3-*O*-isopropylidene-*L*-threitol affording compound **11b** in 5 steps and 16.5% overall yields.

2.2. Antimalarial Activities

All our novel derivatives were tested against *Pf* growth in cell cultures (3D7 strain). Assays were performed by adding compounds on *Pf*-infected erythrocytes suspended in complete medium during 48 hours (one full *Pf* asexual cycle) before assessing parasite viability (Table 1).

It should be noted that, since we tested highly polar and charged compounds on infected RBC cultures, their uptake into both the erythrocyte and the parasite is unlikely to occur via passive diffusion. The ANPs designed by Smeijsters et al.[9] were previously shown to be active in parasite cultures, leading to the hypothesis that an alternative pathway exists through which small polar compounds can enter RBCs. In fact, *Plasmodium* relies on specific channels in the infected-RBC membrane known as new permeation pathways (NPPs) to facilitate the uptake of molecules of low molecular weight, such as carbohydrates, nucleosides, nucleobases, ions, etc., in order to supply the needed material for the parasite development. [25–27] In addition,

Table 1. Activities of ANP derivatives on *P. falciparum* growth (3D7 strain).

Compounds	Nucleobase	Chain length	α	β	γ	IC_{50} (μM)[a] *Pf*
1	**2-amino-6-chloropurine**	C4	H	OH (*R*)	H	**38.8 ± 4.7**
2	2-amino-6-thiopurine	"	"	"	"	>100
3	2-amino-6-chloro-7-deazapurine	"	"	"	"	>100
4	**2-amino-6-oxo-7-deazapurine**	"	"	"	"	**22.2 ± 0.7**
5	2-fluoro-6-oxopurine	"	"	"	"	443.3 ± 107.3
6	Guanine	**C5**	H	OH (*R*)	H	**34.3 ± 9.9**
7	"	C5	"	H	OH (*R*)	>>100
8	"	C4	H	C = O	H	>>100
9	"	C4	H	$P(ONa)_2$	H	>>100
10	"	C4	**OH (*R*/*S*)**	**OH (*S*/*R*)**	H	**11.3 ± 1.1**
11	"	C4	H	OH (*S*/*R*)	OH (*R*/*S*)	>100
11a	Guanine	C4	H	OH (*R*)	OH (*S*)	>1000
11b	Guanine	C4	H	OH (*S*)	OH (*R*)	260.0 ± 30.0
12	Guanine	C4	H	**double bond**		**24.6 ± 3.9**
Chloroquine				/		0.014 ± 0.002

[a] Values are the means of at least three independent experiments performed in duplicate (±SEM).

we showed that our lead compound (UA2239) enters infected RBCs through NPPs,[15] and we assumed that the ANPs tested here may be able to use the same route of entry.

Even if some compounds were found modestly active (**1**, **4**, **6**, **10** and **12**) with IC_{50} values ranging from 11.3 to 38.8 μM, none of them can compete with our lead compound (UA2239, IC_{50} = 74 nM).[14] However, some conclusions and hypotheses could be drawn from these results.

Modification of the guanine moiety always resulted in a decrease of the activity, as already observed in our previous work (Figure 1), but the replacement of the oxygen atom at position 6 with a sulfur atom (Table 1, compound **2**) resulted in a complete loss of the activity. In term of interaction, while oxygen is a strong hydrogen bond acceptor, sulfur is a much weaker one due to its larger size (the van der Waals radius of O is 1.4 Å, compared to 1.9 Å for S) and lower electronegativity. In terms of electronic and steric effects, the C = S bond is longer and weaker than C = O, with a different electronic distribution that could be responsible for the lower affinity of the compound toward the targeted protein. To a lesser extent, a similar steric clash could be responsible for the lower activity of the halogenated compound **1**, which is still retaining μM activity. We should also point out here that the chlorine atom or the sulfur atom in position 6 of a purine ring might be converted to 6 oxo derivative in biological media,[28–30] but this conversion may not be efficient enough in our experimental conditions. Interestingly, the 7-deazaguanine derivative **4** retains some activity (while compound **3** is inactive); this result indicates that the nitrogen atom at position 7 of the purine ring is mandatory to ensure high affinity with the targeted protein. A similar remark can be made concerning the amino group in position 2, as compound **5** (incorporating 2-fluoro-6-oxopurine) also lacks activity.

Chain length modification displayed modest to no antimalarial activities (Table 1, compounds **6** and **7**), whatever the position of the hydroxyl group, indicating that the chain is simply too long for the compound to fit correctly.

The importance of the hydroxyl group in the β-position is also highlighted by the inactive compounds **7**, **8,** and **9**. The carbonyl group is no longer a hydrogen bond donor and could reduce conformations flexibility (sp^2-hybridized carbon). Both of these modifications could impact the affinity between the compound and its target. For the compounds including a diol functionality (i.e., derivatives **10**, **11**, **11a,** and **11b**), only compound **10** exhibited some anti-plasmodial activity, with the lowest IC_{50} value of 11.3 μM of the studied ANPs, thus showing that hydroxyl groups are tolerated in the α- and β-positions.

Finally, the allyl compound (E)-**12** was found moderately active, suggesting (as in our previously published work for ANP containing a vinyl phosphonate group)[14] that the hydroxyl group is an important feature to observe good affinity toward the targeted protein.

2.3. In Silico Docking Studies

We recently proposed that compound UA2239 could act as a potent inhibitor of *Plasmodium falciparum* guanylate cyclase (*Pf*GCα).[15] With the aim to rationalize the differences of activities of UA2239 and its structural analogues, a set of derivatives were docked using PLANTS1.2 [31] in a model of the guanylate cyclase domain of *Pf*GCα generated with AlphaFold2[15,32] and using 2′-deoxy-3′-AMP bound to the cyclase domain of the mammalian adenylate cyclase MamAC (PDB 1CS4) as an anchor. The best-ranked pose (in terms of affinity) of each analogue was selected to be compared to the best UA2239 pose.

The docking of UA2239 highlighted several interactions between *Pf*GCα and our hit compound (Figure 4). The nucleobase is anchored thanks to hydrogen bonding of both guanine C2 and N1 amino groups with Glu3058 acid side-chain (2.7 &

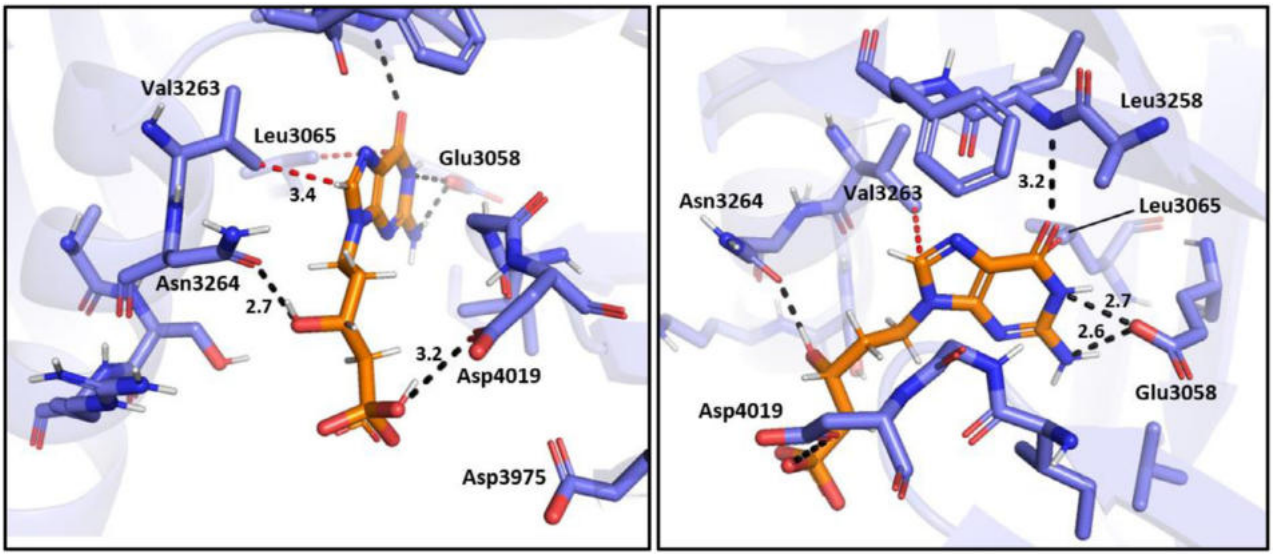

Figure 4. Predicted interactions of UA2239 with residues in the PfGCα guanylate cyclase domain.[a]
[A] UA2239 carbon atoms are represented in orange, and, *Pf*GCα residues, carbon atoms are in violet. Black dotted lines represent hydrogen bonds. Hydrophobic interactions are shown in red dots. Interaction lengths are in Angstrom.

2.6 Å), and of guanine in C6 position with the main-chain NH group of Leu3258 (3.2 Å). The phosphonate group is docked in a wide pocket surrounded by two Asp residues (Asp 4019 and Asp 3975) and the monocharged form of the phosphonate group seems to share a hydrogen bound with Asp4019 (3.2 Å). The hydroxyl group of the aliphatic chain of UA2239 shares a hydrogen bound with Asn3264 amide side chain (2.7 Å). Finally, the guanine moiety is stabilized by hydrophobic interactions with the side chains of Val3263 and Leu3065 (3.4 and 4.2 Å).

From the UA2239 docking data, it seems clear that modification of the nucleobase will impact affinity, since an amino group at the C6 position (as in adenine or diamino purine) or an oxo-group at C2 position (as in xanthine) could not share similar interactions with the surrounding residues of the guanylate cyclase domain. This is emphasized in our docking studies of nucleobase-modified UA2239 analogues (previously described in Figure 1[14] and the ones synthesized herein, Figure 2). Indeed, the adenine derivative (Figure S1, panel E) and the diamino purine derivative (Figure S1, panel D) do not align at all with UA2239 nucleobase. The xanthine derivative (Figure S1, panel C) and the 2-fluoro derivative **5** (Figure S1, panel B) align well, but the oxo/fluoro group at C2 position cannot establish interactions with Glu3058. Furthermore, the highly electronegative fluorine atom at position 2 lowers the electron density of the carbonyl in position 6, thus weakening its hydrogen bonds with Leu3258. This conclusion is highly correlated to our biological assays, since all analogues which do not incorporate guanine as a nucleobase were found inactive (Figure 1 & Table 1).

6-Chloropurine derivative **1** (Figure S1, panel F) does not align at all, mainly due to steric hindrance and hydrophobicity. In addition, the replacement of a carbonyl group (C = O) with chlorine at position 6 of a purine ring has significant electronic effects. The C = O is a strong hydrogen bond acceptor; it is polarized with a partial positive charge on carbon, whereas the chlorine atom (very poor hydrogen bond acceptor) is primarily electron-withdrawing through a strong inductive effect and does not allow the tautomerization. The chlorine also exerts an important impact on the electron density of the purine ring as it withdraws electron density more strongly through induction than carbonyl. This makes the purine ring more electron-deficient overall. In this particular case, it may also be possible that the 6-chloropurine undergoes chemical modification in cells to form its 6-oxo-counterpart and thus compound **1** displays nonetheless a micromolar IC_{50}. Finally, 7-deaza derivative **4** (Figure S1, panel A) is well-aligned, but affinity may suffer from the clash between the hydrophobic C7 carbon atom and the close oxygen atom of Leu3258 main chain (2.7 Å), explaining thus its higher IC_{50} value (22.2 µM) compared to UA2239 (Table 1). Moreover, replacing nitrogen in position 7 with C-H impacts the electron density distribution across the purine ring system, thus affecting hydrogen bonding.

Modification of chain length hinders the docking of the concerned derivatives. C3-chain compounds are too short for the phosphonate group and the hydroxyl group to align well on UA2239 pose (although the pose of the *R*-isomer is quite satisfactory in itself, (Figure S1, panels I & J), and C5-chain compounds **6** and **7** (Figure S1, panel H) are too long, pushing the phosphonate group away from Asp residues. It is assumed that IC_{50} value of C5-chain β-OH derivative **6** is lower than γ-OH compound **7** because of the more suitable location of the hydroxyl group, directed toward Asn3264.

Chemical modification of the chain also has noticeable consequences on the positioning of the corresponding derivatives. The amino group of the β-amino analogue of UA2239 (Figure S1, panel M) does not align with UA2239, possibly because of steric hindrance. The same observations were made for the β-keto compound **8** (Figure S1, panel G), bisphosphonate compound **9** (Figure S1, panels P & Q), bis-hydroxylated compound **11a** (Figure

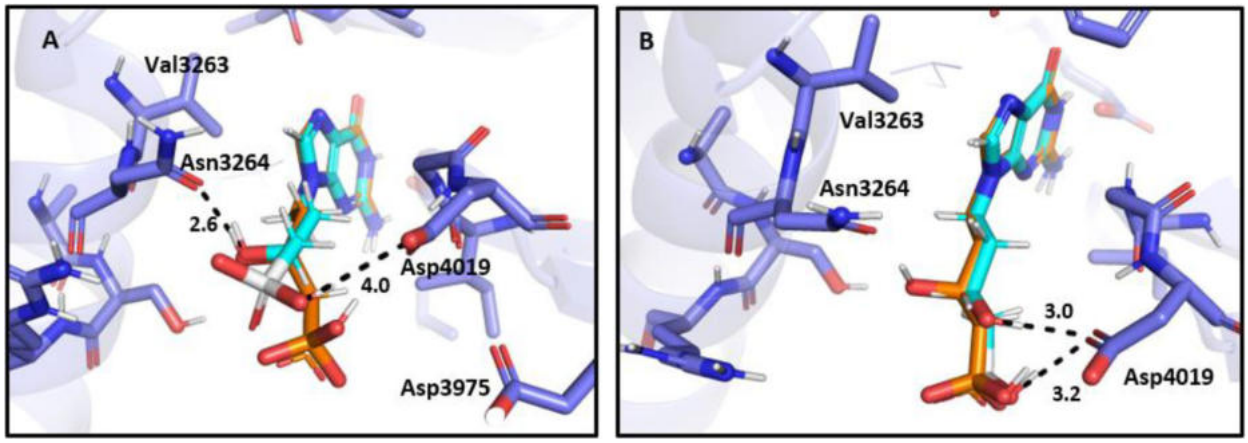

Figure 5. Predicted interactions of the S-isomer of UA2239 with residues in the PfGCα guanylate cyclase domain.[a]
[A] Shown distance is in Angstrom. Dotted lines show distances, not hydrogen bonds. UA2239 carbon atoms are represented in orange, and carbon atoms of the *S*-isomer in cyan. (A) Pose 1 of the docked *S*-isomer, showing the poorly oriented phosphonate group. (B) Pose 2 of the docked *S*-isomer showing the hydroxyl group oriented toward Asp4019 and not Asn3264, as in UA2239.

S1, panel L), and allyl derivative **12** (Figure S1, panel R), because of either steric hindrance (as for compounds **9, 11a,** and β-amino compounds), lack of flexibility (as for compound **12**), or the lack of a hydrogen donor group close to Asn3264 (as for compounds **8** and **12**). All these compounds were found to be biologically inactive, or at best much less active than UA2239. On the other hand, the alkyl derivative (Figure S1, panel T) aligns quite well and shows some activity (micromolar range), highlighting the negative impact of the absence of the hydroxyl group (Table 1). The α, β-bis-hydroxylated compounds **10** fit quite well (Figure S1, panel N), but both isomers suffer from weaker interactions with the surrounding residues compared to UA2239 pose. αR, βS compound does not share a hydrogen bond with Asn3264 since both hydroxyl groups are oriented toward Asp4019 (3 and 3.3 Å, respectively), and the phosphonate group of αS, βR compound is misoriented, possibly because of the steric hindrance associated with the α-OH group. These observations could be correlated to their weaker inhibitory effect (Table 1). The β, γ-bis-hydroxylated compound **11b** aligned quite well with UA2239 (in a striking opposition with compound **11a**), with γ-hydroxyl group pointing toward Asn3264 (2.8 Å), and β-hydroxyl group pointing toward Asp4019 (3 Å), as the phosphonate (Figure S1, panel K). Its high IC_{50} value (260 µM), however, not even close to compound **10**, does not correlate with our observations. Either our docking method has proved its limitations, or unknown pharmacokinetic mechanisms are responsible for the low biological activity of compound **11b**.

Finally, the two best poses of the docked *S*-isomer of compound UA2239 (Figure 5) show that the hydroxyl group must point away from Asn3264 for the phosphonate group to be aligned on the UA2239 pose, or the phosphonate group must move away from Asp4019 to enable the hydrogen bonding between the hydroxyl group and Asn3264 (Figure 5.). Both situations may explain why the *S*-isomer is much less active (6.1 µM) than its *R*-isomer (UA2239).

Overall, these results strongly suggest a correlation between the chemical features of our lead (UA2239, guanine as a nucleobase, β-hydroxyl group, *R*-stereochemistry, C4 chain length, phosphonate group) and a noticeable inhibitory activity against *Pf* growth. It also corroborates our hypothesis that *Pf*GCα is likely the target of UA2239.

3. Conclusion

We reported and tested 14 different and novel ANPs obtained through original synthetic pathways. Our compounds are one of the first nucleotide analogues to be reported as being active as phosphonate (and do not require the systematic use of a pro-drug strategy) against *Pf* in vitro, with EC_{50} in the µM range. However, despite our synthetic effort, none of the novel derivatives competed with our initial lead compound. The presence of the guanine nucleobase, the butyl chain, and the hydroxyl group in the β-position appeared mandatory to observe potent in vitro anti-plasmodial activity. These results agree with the docking studies performed on a *Pf*GCα AlphaFold2-generated model, emphasizing the probability of targeting this enzyme with UA2239, as already reported in our recent work.[15] Differences of biological activity between all tested analogues may be due to a low affinity of the compounds studied with the putative target of UA2239 and/or to a default in the ability of these polar and negatively charged derivatives to cross efficiently both the RBC and the parasitic membranes. Further insights into the detailed mechanism of action of our lead compound will be necessary to envisage further synthetic work in this series.

Supporting Information

The following files are available free of charge. Spectral data (NMR) for intermediates and for final compounds (two separated PDF files). Experimental section for Chemistry, Biological evaluation and Docking study, Snapshots of docking poses of

biologically tested analogues as Figure S1 (PDF file). Additional references cited within the Supporting Information.[19,33,34]

Acknowledgments

We are grateful to the CNRS (National Scientific Research Council) and University of Montpellier for financial support. Analyses were carried out at "PAC Chimie Balard", analytical facilities of Univ Montpellier, CNRS, ENSCM.

N. V. is particularly grateful to the Région Occitanie Pyrénées-Méditerranée for her fellowship. T.C. and Y. B. are grateful to the ANR for their post-doctoral and master fellowships.

Author Contributions

The manuscript was written through contributions of all authors. SP & TC designed the synthesis and NMR studies. TC, NV, and YB performed the chemical experiments. SW & RC designed the biological studies. SW performed the biological experiments. CL and TC performed the docking studies. All authors have given approval to the final version of the manuscript.

Funding Sources

This work is part of the research project "NAN-Pal" supported by the Région Occitanie Pyrénées-Méditerranée and SATT AxLR, and ANR (Agence Nationale pour la Recherche), project PAMalaD (ANR-21- CE18-0057-01).

Conflict of Interest

The authors declare no conflict of interest.

Data Availability Statement

The data that support the findings of this study are available as supplementary material

Keywords: antiprotozoal agents · drug discovery · egress · malaria · nucleotides

[1] WHO, *Vol. 2025*, https://www.who.int/teams/global-malaria-programme/reports/world-malaria-report-2023, **2023**.
[2] R. M. Packard, *New Engl. J. Med.* **2014**, *371*, 397; https://doi.org/10.1056/NEJMp1403340.
[3] P. G. Mathenge, S. K. Low, N. L. Vuong, M. Y. F. Mohamed, H. A. Faraj, G. I. Alieldin, R. Al khudari, N. A. Yahia, A. Khan, O. M. Diab, Y. M. Mohamed, A. H. Zayan, G. M. Tawfik, N. T. Huy, K. Hirayama, *Parasitol. Int.* **2020**, *74*, 101919; https://doi.org/10.1016/j.parint.2019.04.016.
[4] K. E. Ward, D. A. Fidock, J. L. Bridgford, *Curr. Opin. Microbiol.* **2022**, *69*, 102193. https://doi.org/10.1016/j.mib.2022.102193.
[5] M. Quagliata, A. M. Papini, P. Rovero, *Expert Opin. Ther. Patents* **2023**, *33*, 169; https://doi.org/10.1080/13543776.2023.2190884.
[6] A. Nadeem, W. Bilal, *Asian Pacif. J. Trop. Med.* **2023**, *16*, 162. https://doi.org/10.4103/1995-7645.374354.
[7] Y. Y. Syed, *Drugs Ther. Persp* **2022**, *38*, 373. https://doi.org/10.1007/s40267-022-00937-3.
[8] E. De Clercq, *Viruses* **2022**, *14*, 1978. https://doi.org/10.3390/v14091978.
[9] L. J. J. W. Smeijsters, F. F. J. Franssen, L. Naesens, E. de Vries, A. Holý, J. Balzarini, E. de Clercq, J. P. Overdulve, *Int. J. Antimicrob. Agents* **1999**, *12*, 53. https://doi.org/10.1016/S0924-8579(99)00003-5.
[10] T. Cheviet, I. Lefebvre-Tournier, S. Wein, S. Peyrottes, *J. Med. Chem.* **2019**, *62*, 8365; https://doi.org/10.1021/acs.jmedchem.9b00182.
[11] J. Frydrych, D. T. Keough, H. Xia, L. P. Slavětínská, M. Dračínský, M. Česnek, J. Travis, M. Chavchich, M. Edstein, D. Hocková, L. W. Guddat, Z. Janeba, *ChemMedChem* **2025**, *20*, e202500575; https://doi.org/10.1002/cmdc.202500575.
[12] D. T. Keough, M. Petrová, G. King, M. Kratochvíl, R. Pohl, E. Doleželová, A. Zíková, L. W. Guddat, D. Rejman, *J. Med. Chem.* **2024**, *67*, 7158; https://doi.org/10.1021/acs.jmedchem.4c00021.
[13] Y. V. T. Minnow, K. Suthagar, K. Clinch, R. G. Ducati, A. Ghosh, J. N. Buckler, R. K. Harijan, S. M. Cahill, P. C. Tyler, V. L. Schramm, *ACS Chem. Biol.* **2022**, *17*, 3407. https://doi.org/10.1021/acschembio.2c00546.
[14] T. Cheviet, S. Wein, G. Bourchenin, M. Lagacherie, C. Périgaud, R. Cerdan, S. Peyrottes, *J. Med. Chem.* **2020**, *63*, 8069. https://doi.org/10.1021/acs.jmedchem.0c00131.
[15] M. Ali, R. Dura, M.-A. Guery, E. Colard-Itté, T. Cheviet, L. Robresco, L. Berry, C. Lionne, C. Lavazec, A. Claessens, S. Peyrottes, K. Wengelnik, S. Wein, R. Cerdan, *Sci. Adv. in press*.
[16] D. T. Keough, P. Spacek, D. Hockova, T. Tichy, S. Vrbkova, L. Slavetinska, Z. Janeba, L. Naesens, M. D. Edstein, M. Chavchich, T. H. Wang, J. de Jersey, L. W. Guddat, *J. Med. Chem.* **2013**, *56*, 2513; https://doi.org/10.1021/jm301893b.
[17] P. Spacek, D. T. Keough, M. Chavchich, M. Dracinsky, Z. Janeba, L. Naesens, M. D. Edstein, L. W. Guddat, D. Hockova, *J. Med. Chem.* **2017**, *60*, 7539; https://doi.org/10.1021/acs.jmedchem.7b00926.
[18] P. Spacek, D. T. Keough, M. Chavchich, M. Dracinsky, Z. Janeba, L. Naesens, M. D. Edstein, L. W. Guddat, D. Hockova, *Bioorg. Med. Chem.* **2017**, *25*, 4008. https://doi.org/10.1016/j.bmc.2017.05.048.
[19] C. R. Coxon, E. Anscombe, S. J. Harnor, M. P. Martin, B. Carbain, B. T. Golding, I. R. Hardcastle, L. K. Harlow, S. Korolchuk, C. J. Matheson, D. R. Newell, M. E. M. Noble, M. Sivaprakasam, S. J. Tudhope, D. M. Turner, L. Z. Wang, S. R. Wedge, C. Wong, R. J. Griffin, J. A. Endicott, C. Cano, *J. Med. Chem.* **2017**, *60*, 1746. https://doi.org/10.1021/acs.jmedchem.6b01254.
[20] Y. Gao, T. Kodadek, *Chem. Biol.* **2013**, *20*, 360. https://doi.org/10.1016/j.chembiol.2013.01.013.
[21] M. Kasthuri, C. El Amri, V. Lefort, C. Périgaud, S. Peyrottes, *New J. Chem.* **2014**, *38*, 4736; https://doi.org/10.1039/C4NJ00813H.
[22] M. Kasthuri, L. Chaloin, C. Périgaud, S. Peyrottes, *Tetrahedron: Asymmetry* **2011**, *22*, 1505. https://doi.org/10.1016/j.tetasy.2011.08.010.
[23] L. Wang, K. B. Sharpless, *J. Am. Chem. Soc.* **1992**, *114*, 7568. https://doi.org/10.1021/ja00045a042.
[24] D. Topalis, U. Pradère, V. Roy, C. Caillat, A. Azzouzi, J. Broggi, R. Snoeck, G. Andrei, J. Lin, S. Eriksson, J. A. C. Alexandre, C. El-Amri, D. Deville-Bonne, P. Meyer, J. Balzarini, L. A. Agrofoglio, *J. Med. Chem.* **2011**, *54*, 222. https://doi.org/10.1021/jm1011462.
[25] H. Ginsburg, W. D. Stein, *J. Membr. Biol.* **2004**, *197*, 113; https://doi.org/10.1007/s00232-003-0646-7.
[26] H. Ginsburg, M. Krugliak, O. Eidelman, Z. I. Cabantchik, *Mol. Biochem. Parasitol.* **1983**, *8*, 177; https://doi.org/10.1016/0166-6851(83)90008-7.
[27] S. Baumeister, J. Wiesner, A. Reichenberg, M. Hintz, S. Bietz, O. S. Harb, D. S. Roos, M. Kordes, J. Friesen, K. Matuschewski, K. Lingelbach, H. Jomaa, F. Seeber, *PLoS One* **2011**, *6*, e19334. https://doi.org/10.1371/journal.pone.0019334.
[28] D. E. Duggan, E. Titus, *J. Biol. Chem.* **1959**, *234*, 2100; https://doi.org/10.1016/S0021-9258(18)69873-4.
[29] G. B. Elion, S. Callahan, H. Nathan, S. Bieber, R. W. Rundles, G. H. Hitchings, *Biochem. Pharmacol.* **1963**, *12*, 85; https://doi.org/10.1016/0006-2952(63)90012-1.
[30] I. Y. Hwang, A. A. Elfarra, *J. Pharmacol. Exper. Ther.* **1993**, *264*, 41. https://doi.org/10.1016/S0022-3565(25)10284-X.
[31] O. Korb, T. Stützle, T. E. Exner, in *Ant ColonyOptimization and SwarmIntelligence* (Eds.: M. Dorigo, L. M. Gambardella, M. Birattari, A. Martinoli, R. Poli, T. Stützle), Springer Berlin Heidelberg, Berlin, Heidelberg, **2006**, pp. 247–258.

[32] J. Jumper, R. Evans, A. Pritzel, T. Green, M. Figurnov, O. Ronneberger, K. Tunyasuvunakool, R. Bates, A. Žídek, A. Potapenko, A. Bridgland, C. Meyer, S. A. A. Kohl, A. J. Ballard, A. Cowie, B. Romera-Paredes, S. Nikolov, R. Jain, J. Adler, T. Back, S. Petersen, D. Reiman, E. Clancy, M. Zielinski, M. Steinegger, M. Pacholska, T. Berghammer, S. Bodenstein, D. Silver, O. Vinyals, A. W. Senior, K. Kavukcuoglu, P. Kohli, D. Hassabis, *Nature* **2021**, *596*, 583. https://doi.org/10.1038/s41586-021-03819-2.
[33] M. L. Ancelin, M. Calas, V. Vidal-Sailhan, S. Herbuté, P. Ringwald, H. J. Vial, *Antimicrob. Agents Chemother.* **2003**, *47*, 2590. https://doi.org/10.1128/AAC.47.8.2590-2597.2003.
[34] R. E. Desjardins, C. J. Canfield, J. D. Haynes, J. D. Chulay, *Antimicrob. Agents Chemother.* **1979**, *16*, 710. https://doi.org/10.1128/AAC.16.6.710.

Manuscript received: September 15, 2025
Revised manuscript received: October 23, 2025
Version of record online: ■■, ■■